RESEARCH ARTICLE | JULY 01 2013

# Room temperature terahertz quantum cascade laser sources with 215 μW output power through epilayer-down mounting

Q. Y. Lu; N. Bandyopadhyay; S. Slivken; Y. Bai; M. Razeghi



*Appl. Phys. Lett.* 103, 011101 (2013)
https://doi.org/10.1063/1.4812814

APPLIED PHYSICS LETTERS 103, 011101 (2013)

# Room temperature terahertz quantum cascade laser sources with 215lW output power through epilayer-down mounting

Q. Y. Lu, N. Bandyopadhyay, S. Slivken, Y. Bai, and M. Razeghi[a)]
Center for Quantum Devices, Department of Electrical Engineering and Computer Science, Northwestern University, Evanston, Illinois 60208, USA

(Received 29 April 2013; accepted 16 June 2013; published online 1 July 2013)

We report room temperature terahertz (THz) quantum cascade laser sources with high power based on difference frequency generation. The device is Cerenkov phase matched and spectrally purified with an integrated dual-period distributed-feedback grating. Symmetric current injection and epilayer-down mounting of the device onto a patterned submount are used to improve the electrical uniformity and heat removal, respectively. The epilayer-down mounting also allows for THz anti-reflective coating to enhance the THz outcoupling efficiency. Single mode emission at 3.5 THz with a side-mode suppression ratio and output power up to 30dB and 215lW are obtained, respectively.  [http://dx.doi.org/10.1063/1.4812814]

Although the terahertz (THz) spectrum is suited for many applications, such as medical imaging, material characterization, and biological sensing, the practical utilization of this spectrum has been underdeveloped largely due to the lack of compact, high power THz source. While the THz quantum cascade lasers (QCLs) have emerged as the most powerful semiconductor THz sources in the 2–5 THz range,[1] the operational temperature is still below 200K[2] which is difficult to access with thermoelectric coolers. On the other hand, the based-InP QCLs in the mid-infrared (mid-IR) frequency range have gained significant advancements in the recent years in terms of power and efficiency.[3–6] The THz source based on intracavity difference-frequency generation (DFG) from the mid-IR QCLs is free from the temperature issue that is suffered by the THz QCLs, hence room temperature operation is readily demonstrated.[7]

With further improvement by incorporating integrated dual-period distributed-feedback (DFB) grating[8] into the waveguide to purify and tune the mid-IR as well as the THz spectra and Cerenkov phase-matching scheme [9] to enhance the THz outcoupling efficiency, the performance of this type of THz QCL sources is continually improving. Room temperature THz output power of 215lW is demonstrated with Cerenkov phase matching.

Figures 1(a) and 1(b) show the temperature and electrical potential distributions of an epilayer-up mounted QCL with an asymmetric contact pattern (single-sided current injection) near the front facet. The x, y, and z directions are the lateral, longitudinal, and growth directions, respectively. The polished angle of the facet is set to be 30. The thermal conductivities of the materials are from Ref. 12 and the heat source density is set to be $2.5 10^6$ W/cm$^3$ considering the average input power at 1% duty cycle. The electrical conductivities of bulk materials are from Ref. 13 and the electrical conductivity of the active region in the growth direction is fitted from the current-voltage (I-V) curve of a reference device. Clearly, the Cerenkov device suffers severely from both thermal and electrical issues, as the heat near the front facet is not effectively dissipated and the non-uniform electrical distribution across the active region induces nonuniform current injection with the electrical field varying over 2–4kV/cm. In order to address these two issues, we design and demonstrate double-sided current injection and

perature single-mode operation covering an extremely wide THz spectral range of 1–4.6 THz with maximum power up to 32lW and mid-IR to THz conversion efficiency g¼50lW/W$^2$ has been demonstrated.[10] Here, g¼$W_{THz}$/ ($W_1W_2$), with $W_{THz}$ and $W_i$ (i¼1, 2 denoting the two midIR wavelength), defined as the THz power and mid-IR power, respectively. Even higher THz power has been obtained from the collinearly modal-phase matched THz QCL sources at 4 THz, with THz output power up to 65lW and g¼23lW/W$^2$.[11] Despite a higher conversion efficiency, the THz power of the Cerenkov phase-matched device was lower than the modal phase-matched device due to a poorer heat removal mechanism and a less efficient current injection scheme. In this work, these limitations are circumvented by epilayer-down mounting and a symmetric contact pattern. As

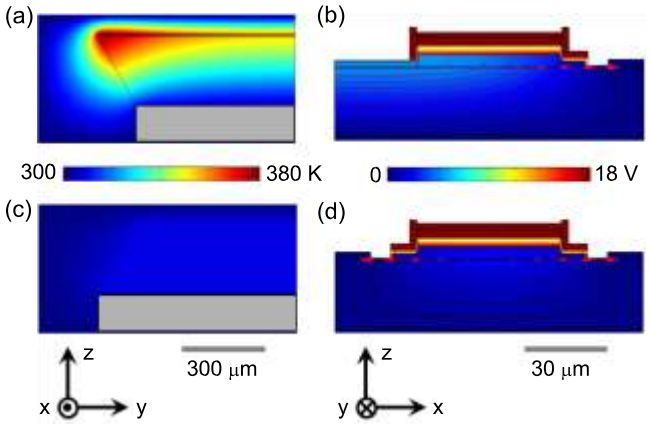


FIG. 1. Temperature and electrical potential distributions of devices with epilayer-up (a) and (b), and epilayer-down mounting schemes (c) and (d). The lines and arrows in (b) and (d) denote the contour lines of the electrical potential and the current flow. Current injection is single-sided in (b) and double-sided in (d).

a)Electronic mail: razeghi@eecs.northwestern.edu

0003-6951/2013/103(1)/011101/4/$30.00 103, 011101-1 

epilayer-down mounting on a submount. Figs. 1(c) and 1(d) show the temperature and electrical potential distributions of a device with epilayer-down mounting to a diamond submount. The heat dissipation is improved significantly and the electrical distribution is much more uniform with electrical field variation less than 0.5kV/cm in the x-z plane of the active region.

The QCL structure is based on the single phonon resonance (SPR) dual-core structure[10,14] with the lattice-matched $In_{0.53}Ga_{0.47}As/In_{0.52}Al_{0.48}As$ laser core grown by gas-source molecular beam epitaxy on a semi-insulating InP substrate. The average doping of the active region is 5.2$10^{16}$ cm$^3$. The waveguide structure is similar to that in Ref. 10, except that the thickness of the InP bottom contact layer (Si, 1$10^{18}$ cm$^3$) is reduced from 1lm to 0.25lm, the InP buffer layer (Si, 2$10^{16}$ cm$^3$) from 5lm to 3lm, and the InP top cladding layer (Si, 2$10^{16}$ cm$^3$) from 3.5lm to 3.2lm. The reduced top cladding layer helps increase the dual-period DFB coupling strength, which is important for the stable dual wavelength operation with a wide THz frequency spacing. The reduced bottom contact layer and buffer layer thicknesses increase the THz transmission from the active regions to the InP substrate by about a factor of 2.

For the Cerenkov devices in Refs. 9 and 10, the top and bottom contacts are on the same side. A gap has to be defined along the ridge to isolate the two contacts. To improve the uniformity of the current injection, two bottom contacts together with two contact gaps are fabricated on the two sides of the ridge waveguide. Unfortunately, the limited area of the ridge isolated by the two gaps makes it difficult for normal wire bonding. As a result, submounts with the corresponding patterns have to be prepared for the epilayer-down mounting.

The sample is processed into double-channel geometries with a ridge width of 20lm. The 1.5-mm long DFB section is patterned with a dual-period grating within a 3mm long laser cavity. The frequency spacing of the grating targets 3.5 THz. This frequency is of special interest to studies of global warming and ozone destruction since the hydroxyl (OH) radical has a strong spectral line at this frequency.[15] The grating is defined by electron beam lithography and transferred to the top contact layer with a standard plasma etching step. The coupling coefficients (j) for the two wavelengths are about 15–20cm$^1$. For comparison, part of the sample is processed with one bottom contact for testing with epilayer-up mounting. The substrate is polished without lapping to keep the maximum thickness around 340lm. After this, the laser bar is high-reflection (HR) coated with $Si_3N_4$/Au (400/100nm).

Both epilayer-up and epilayer-down mounted devices were characterised at room temperature for comparison. The substrate near the front facet has been polished at 25 with respect to the normal cleavage plane without damaging the mid-IR facet in order to collect the THz signal which satisfies the Cerenkov phase-matching scheme. The mid-IR out- put power in pulsed mode operation with 1% duty cycle was measured using a calibrated thermopile detector. The mid-IR spectra were taken in rapid scan mode at a resolution of 0.125cm$^1$ from a Bruker Fourier transform infrared (FTIR) spectrometer equipped with a mid-IR deuterated L-alanine doped triglycine sulfate (DTGS) detector. The power-

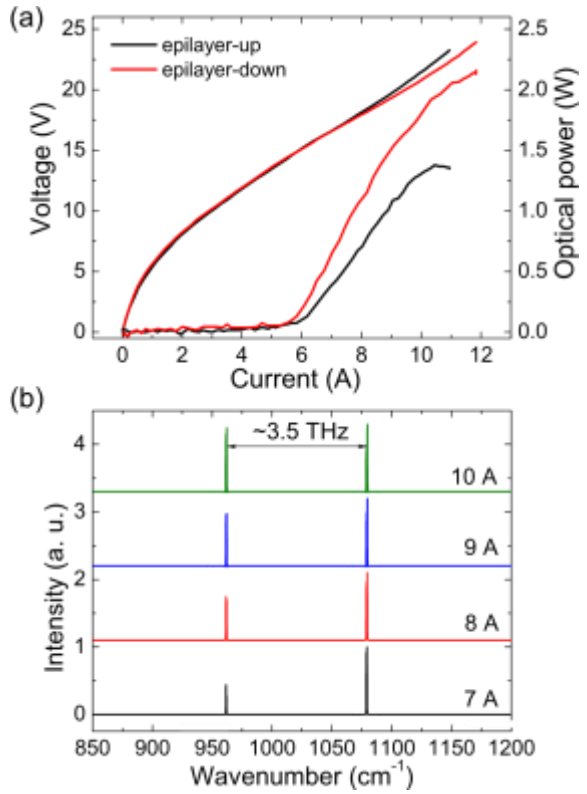


FIG. 2. (a) Mid-IR P-I-V and (b) spectra characterizations at different currents for the epilayer-up and -down mounted devices.

current-voltage (P-I-V) characterizations of two devices with different mounting schemes are shown in Fig. 2(a). The epilayer-down mounted device exhibits reduced threshold current density and voltage with 35% higher mid-IR power compared with its epilayer-up counterpart. The mid-IR spectra of the epilayer-down device in Fig. 2(b) exhibits stable dual-wavelength emissions at $k_1$ ¼9.26lm and $k_2$ ¼10.4lm in the working current range. Similar spectral behavior is also observed from the epilayer-up device.

For the THz characterization, a calibrated Golay cell detector and an uncooled far-IR DTGS detector are used for the THz power and spectrum measurements. Optical filters were used to differentiate the THz power from mid-IR powers. No hyperhemispherical micro Si lens or parabolic mirrors are used to collect the power. THz power was corrected by a collection efficiency of 50% according to the THz far field pattern, the aperture of the detector (6mm), and the distance between the laser and detector (15mm). The far field is obtained with a computer controlled rotational stage and a Golay cell detector placed 5cm away from the laser.

Figure 3(a) shows that THz powers up to 160lW and 70lW with power conversion efficiencies of g¼160 and 148lW/W$^2$ at high currents are obtained for the epilayerdown and epilayer-up mounted devices, respectively. The higher THz power of the epilayer-down mounted device is attributed to the improved thermal and electrical managements. Compared to Ref. 10, the improved conversion efficiency is attributed to the higher THz frequency operation, and increased THz transmission through the reduced thickness of the bottom contact layer. THz far fields in the lateral and vertical directions for the epilayer-down mounted device at a working current of 10A are presented in inset of Fig. 3(a).

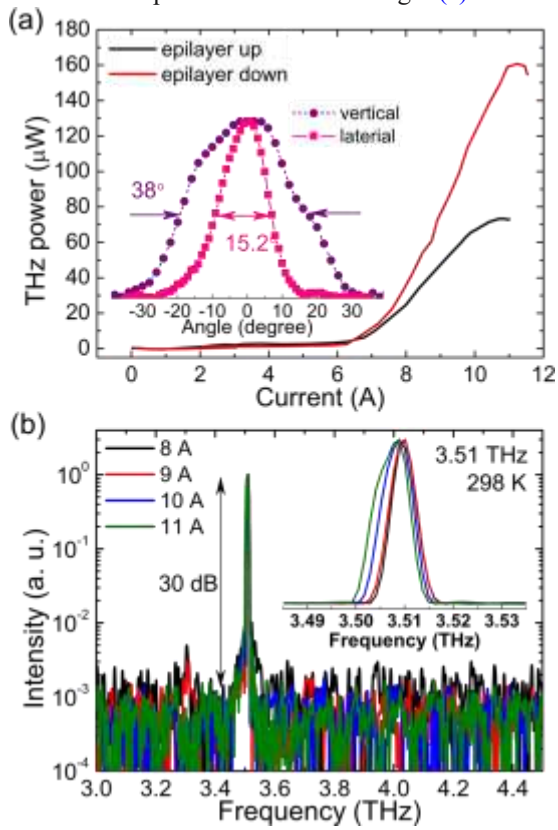


FIG. 3. (a) THz power as a function of current for the devices with two mounting schemes. The inset is the THz far fields of the epilayer-down mounted device at 10A in vertical and lateral directions. (b) THz spectra of the epilayer-down mounted device at different working currents. The inset is the THz spectra in linear scale.

The device exhibits single-lobed beam distributions in both directions with a full width at half maximum (FWHM) of 15.2 and 38, respectively, The THz beam peaks at 0 in both directions. The epilayer-down mounted device exhibits a stable single mode operation around 3.51 THz (k85.5lm), as plotted in Fig. 3(b). The SMSR of the normalized spectra is as high as 30dB at high currents. This is compared with the results in Refs. 10 and 11 with a SMSR as high as 40dB obtained with the liquid-helium cooled silicon bolometer. The lower SMSR here is due to the lower sensitivity of the uncooled far-IR DTGS detector. The THz spectral position is stable as the current changes. The average current tuning rate is about 1GHz/A and the linewidth is about 6–8.6GHz (inset of Fig. 3(b)), which is mainly limited by the resolution of the FTIR spectrometer (0.125cm$^1$). Much wider, continuous tuning can be achieved by employing the dual-section sampled grating design.[16]

All previous Cerenkov implementations share a common feature of preserving the mid-IR facets when forming the inclined facet. For our THz device with distributed feedback mechanism, since the grating feedback (jL4.5–6 for the HR coated cavity with 1.5-mm long grating section) is much stronger than the mirror feedback, the mid-IR threshold is mainly determined by the grating feedback rather than the

mirror feedback. We attempted to extend the polished area through the mid-IR mirror facet. As such, the threshold current increases by about 0.5A, and the mid-IR output power is reduced dramatically to 0.5W. Moreover, the THz

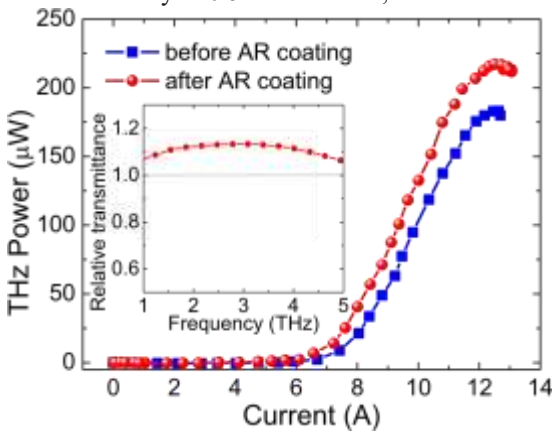


FIG. 4. THz powers characterizations of an epilayer-down mounted device with polished mid-IR facet (blue dotted line) and after applying SU-8 coating (red dotted line). The inset is the relative transmission of a 15-lm thick SU-8 coating on a high-resistivity Si wafer.

power increases to 183lW, as shown in Fig. 4 (blue curve). The nominal THz conversion efficiency is above 2 mW/W$^2$. This behaviour can be explained as follows. The THz signal is generated inside the cavity, so the mid-IR pumping power that is relevant to the nonlinear generation is the mid-IR power flux within the cavity rather than the output power. In this case, even though the mid-IR output power is reduced due to the facet polishing, the forward travelling power flux inside the cavity actually increases due to the reduced inplane reflectivity.

In the epilayer-down mounting scheme, the InP substrate is exposed. Therefore, THz power can be further enhanced by THz anti-reflection (AR) coating. Several materials have been employed as the THz AR coating, such as $SiO_2$, Parylene, and low-density polyethylene.[17,18] Here, SU8 photoresist is used for its simplicity. The inset in Fig. 4 shows the relative transmission of a 15-lm SU-8 layer on a high-resistivity Si wafer. Given a refractive index of 1.7, the absorption loss at 3.5 THz is estimated to be 100cm$^1$, and the optimal coating thickness on InP substrate is around 11lm with a maximum transmission of about 87%. The SU8 photoresist is then spin coated on the mounted device, and baked and cured. The coating thickness is controlled by the spin rate. The THz powers after the SU-8 coating (red curve) are shown in Fig. 4(b). The power is enhanced by 17.5% to 215lW. Ideally, with the low-loss coatings, such as $SiO_2$, or low-density polyethylene, power enhancement above 40% can be achieved, which will be our future work.

In summary, we have demonstrated high power, high efficiency THz QCL sources with a Cerenkov phase-matching scheme by applying the epilayer-down mounting strategy. This mounting technique together with the double-sided current injection design helps to improve the mid-IR and THz performance. A THz AR coating is used to enhance the THz outcoupling efficiency. Room temperature single mode emission at 3.51 THz with output power and SMSR up to 215lW and 30dB are obtained, respectively.

This work is partially supported by the National Science Foundation under grant ECCS-1231289. The authors would also like to acknowledge the encouragement and support of Dr. D. Pavlidis from National Science Foundation, Dr. K.K. Law from the Naval Air Warfare Center, Dr. T. Manzur from the Naval Undersea Warfare Center, and Dr. N. Dhar from the Defense Advanced Research Projects Agency.

[1] B. S. Williams, Nature Photon. 1, 517 (2007).
[2] S. Fathololoumi, E. Dupont, C. W. I. Chan, Z. R. Wasilewski, S. R. Laframboise, D. Ban, A. Matyas, C. Jirauschek, Q. Hu, and H. C. Liu, Opt. Express 20, 3866 (2012).
[3] M. Razeghi, IEEE J. Quantum Electron. 15, 941 (2009).
[4] D. Dey, W. Wu, O. G. Memis, and H. Mohseni, Appl. Phys. Lett. 94, 081109 (2009).
[5] Y. Bai, N. Bandyopadhyay, S. Tsao, S. Slivken, and M. Razeghi, Appl. Phys. Lett. 98, 181102 (2011).
[6] A. Lyakh, R. Maulini, A. Tsekoun, R. Go, and C. K. N. Patel, Opt. Express 20, 24272 (2012).
[7] M. A. Belkin, F. Capasso, F. Xie, A. Belyanin, M. Fischer, A. Wittmann, and J. Faist, Appl. Phys. Lett. 92, 201101 (2008).
[8] Q. Y. Lu, N. Bandyopadhyay, S. Slivken, Y. Bai, and M. Razeghi, Appl. Phys. Lett. 99, 131106 (2011).
[9] K. Vijayraghavan, R. W. Adams, A. Vizbaras, M. Jang, C. Grasse, G. Boehm, M. C. Amann, and M. A. Belkin, Appl. Phys. Lett. 100, 251104 (2012).
[10] Q. Y. Lu, N. Bandyopadhyay, S. Slivken, Y. Bai, and M. Razeghi, Appl. Phys. Lett. 101, 251121 (2012).
[11] Q. Y. Lu, N. Bandyopadhyay, S. Slivken, Y. Bai, and M. Razeghi, Opt. Express 21, 968 (2013).
[12] A. Lops, V. Spagnolo, and G. Scamarcio, J. Appl. Phys. 100, 043109 (2006). [13] C. Becker and C. Sirtori, J. Appl. Phys. 90, 1688 (2001).
[14] Y. Bai, N. Bandyopadhyay, S. Tsao, E. Selcuk, S. Slivken, and M. Razeghi, Appl. Phys. Lett. 97, 251104 (2010).
[15] R. G. Prinn, J. Huang, R. F. Weiss, D. M. Cunnold, P. J. Fraser, P. G.Simmonds, A. McCulloch, C. Harth, P. Salameh, S. O'Doherty, R. H. J. Wang, L. Porter, and B. R. Miller, Science 292, 1882 (2001).
[16] S. Slivken, N. Bandyopadhyay, S. Tsao, S. Nida, Y. Bai, Q. Y. Lu, and M. Razeghi, Appl. Phys. Lett. 100, 261112 (2012).
[17] J. Xu, J. M. Hensley, D. B. Fenner, R. P. Green, L. Mahler, A. Tredicucci, M. G. Allen, F. Beltram, H. E. Beere, and D. A. Ritchie, Appl. Phys. Lett. 91, 121104 (2007).
[18] A. W. M. Lee, Q. Qin, S. Kumar, B. S. Williams, Q. Hu, and J. L. Reno, Opt. Lett. 35, 910 (2010).